ENGINEERING AND ITS APPLICATIONS
VOLUME 3, ISSUE 1, 1–36
ISSN: 3127-5435
https://engineering-journals.org/journals/eia/

Structural Optimization of Heat Transfer Fins in the Energy Storage System Revisited

Fei Xu[a], Jingfei Jiang[a], Haibo Zhou[b], Juan LG Guirao[c]

[a] *Center for Dynamics and Intelligent Control Research, School of Mathematics and Statistics, Shandong University of Technology, ZiBo 255000, China*
[b] *Beijing Key Laboratory of Petroleum Data Mining, China University of Petroleum, Beijing 102249, China*
[c] *Department of Applied Mathematics and Statistics, Technical University of Cartagena, Hospital de Marina, Cartagena 30203, Spain*

Abstract. This revisited study is concerned with exploring a new heat transfer algorithm which is independent of changes in fin geometry and material properties. By applying dynamic programming and differential thinking to recursively calculate the heat transfer between elemental units, this algorithm can quickly calculate the heat transfer characteristics and only relies on the thermal conductivity of the fins. In addition, to more concisely and accurately reflect the heat transfer performance of the thermal energy storage system, this study proposes a new performance evaluation method that comprehensively considers heat transfer speed and the proportion of phase change materials in space. Furthermore, due to the advantage of triangular fins in occupying less space, the heat transfer characteristics of triangular fins were analyzed using a distance field between fins, and it was found that inverted triangular fins have better heat transfer performance. The heat transfer duration of triangular fins with different sizes, layouts, and quantities was calculated using a heat transfer model and experimental methods of coarse and fine sampling, and the performance of different fins was calculated using the new performance evaluation method. The results show that when the height of the inverted triangular fin is 0.029m, the base length is 0.0024m, and the fin angle is $\pi/10$, its heat transfer performance is optimal, with an evaluation value of 3.572. Compared with the optimal parameters of equilateral upright triangular fins, the heat transfer performance of inverted triangular fins is improved by 17.3%; compared with the fixed size rectangular fin parameters, the performance is improved by 103.6%.

1. Introduction

The increasing world energy crisis has promoted the research and development of renewable resources. High energy storage technology is the key technology to solve the fluctuation and indirectness of renewable resources and waste heat resources[14]. Phase change heat storage has become one of the more widely used methods because of its higher heat storage, smaller volume change before and after phase change and stable performance[6, 22]. It has broad application prospects in the field of solar thermal power generation[4].

Corresponding author: Juan LG Guirao, mail address: juan.garcia@upct.es
Received: 10 January 2026; Accepted: 25 June 2026; Published: 20 July 2026.
Keywords. Heat conduction model, Dynamic programming, Evaluation equation, Distance field model, Triangular fins
2010 *Mathematics Subject Classification.* xxxxx, xxxxx, xxxxx
Cited this article as: Xu, F., Jiang, J., Zhou, H., Guirao, J.L.G., Structural Optimization of Heat Transfer Fins in the Energy Storage System, Engineering Journals, *3(1), 2026, 1–36*

Phase change materials (PCMs) are widely used as energy storage media in phase change energy storage technology. Compared to other storage materials, PCMs can store 5-14 times the energy in the same volume and has a lower phase change temperature difference[8]. In addition, the cost of PCMs is relatively low. However, traditional PCM has a low thermal conductivity, which severely limits the application of phase change energy storage technology. Therefore, improving the heat transfer efficiency of PCMs has become a key goal for the development of phase change heat storage technology[1]. Several research methods aim to improve the thermal conductivity of PCMs through material selection, including packaging techniques[15] and the addition of particles with high thermal conductivity[24]. For example, dispersing highly conductive nanoparticles with diameters between 1-100nm can improve the thermal conductivity of PCM[4, 13, 25]. However, this approach reduces the volume percentage of the PCM, resulting in a reduction in heat capacity[5]. Zhang et al.[27] studied a three-dimensional graphite layered porous carbon composite with a high thermal conductivity of 0.88 $W/(m \cdot K)$. In addition, encapsulating PCM into small hollow capsules is also a common technique to increase the contact area between PCM and heat transfer fluid [11]. However, this method has the problems of high production costs and the possibility of rupture of encapsulated hollow capsules, resulting in lower reliability. Phase change heat storage has become a widely used method for storing thermal energy. However, most phase change materials (PCMs) have low thermal conductivity, so enhanced measures are needed to increase the heat transfer rate of phase change energy storage devices. Adding fins in the phase change energy storage system can increase the contact area between the heat transfer boundary and PCMs, and the fins have the advantages of low manufacturing cost, easy use and high heat transfer efficiency, so they are widely used. Therefore, it is of great research significance to optimize the fin structure to achieve rapid heat transfer and improve the heat transfer performance of the heat storage system. The shapes of the fins include V-shaped fins [2], tree-shaped fins[9] , Y-shaped fins[19], snowflake longitudinal fins[20], spiral fins[21], ring fins[7] and so on. Khan et al.[12] compared the ring fin and the longitudinal fin, and found that the heat storage time of the ring fin was better than that of the longitudinal fin, and the melting rate was increased by 18.98%. Pizzolato et al.[18] designed a new type of fin through topology optimization to improve its heat transfer efficiency in the phase change heat storage device, and proposed a new fin layout algorithm to reduce the phase transition time of PCMs, compared to rectangular fins, PCMs melts 37% faster and cures 15% faster. In summary, the geometry of different fins has an important influence on the heat storage time of the phase change heat storage system, and the size and layout of the fins also affect the heat storage efficiency. Ye et al.[26] studied the effects of boundary conditions and fin number on heat storage efficiency, and the results showed that PCMs had the most ideal melting effect when the number of fins was 10. Xingyu and Shouguang [10] used the response surface method to determine the optimal structural characteristics of Fibonacci-based triangular longitudinal fins. including parameters such as width, length and height. Through numerical simulation, the heat transfer characteristics of the casing latent heat storage system during the cooling and curing process were studied. Comprehensive analysis shows that fins with different geometries significantly shorten the heat storage time, while optimizing the size and number of fins can achieve the best heat storage time. However, fins with complex geometries, such as ring fins and tree fins, occupy a lot of PCMs space, resulting in a significant reduction in heat capacity. In contrast, triangular fins have the characteristics of short heat storage time and small proportion of space, so it is of great significance to reasonably design the size and arrangement of triangular fins.

Understanding the real-time heat transfer performance of fins is essential for analyzing heat storage processes. Researching an accurate, concise, and efficient simulation algorithm is not only able to overcome the limitations of expensive experimental equipment but also significantly improve experimental efficiency. Shen et al.[23] developed a two-dimensional numerical model for LHSU and solved it using the SIMPLE algorithm in the FLUENT software. The maximum discrepancy between the experimental and simulation results was 8.22%. Seong et al.[17] employed an enthalpy-porosity model to describe the unsteady flow and heat transfer characteristics during the melting process. They solved the governing equations using the FLUENT software and utilized ANSYS Workbench to generate the geometric shape and mesh of the fins. The difference between their computed results and the experimental results of Muhammad et al.[16] was less than 7.4%.In summary, most studies that employ FLUENT for equation solving and heat transfer simulation exhibit significant errors. Additionally, there is a lack of independence between the governing equations and the generation of geometric structures for phase change heat storage systems, resulting in a poor level of abstraction in the heat transfer models. An excessive number of constrained variables is also one of the primary reasons for the large errors in heat transfer models. Therefore, establishing a heat transfer model that is not limited by geometric shapes, is stable, and achieves high accuracy is of paramount importance.

In conclusion, previous studies have extensively investigated heat transfer models and triangular fins. However, there is limited research on the comprehensive performance analysis of highly abstract heat transfer models, the distribution of triangular fins, and the impact of fin area ratios. Therefore, this study introduces a novel performance evaluation method for phase change heat storage systems, considering the influence of different sizes, shapes, and quantities of fins on heat transfer time and fin area ratios. Additionally, the factors affecting heat transfer of triangular fins are analyzed, and an optimal arrangement for the heat transfer performance of triangular fins is proposed. Furthermore, a new heat transfer model is designed, which overcomes geometric limitations and achieves stability and high accuracy by employing differential principles and utilizing a minimal number of variables to simulate heat transfer processes.

2. Numerical simulation

This chapter provides a detailed description of the numerical design of a phase change thermal energy storage system. The first section introduces the tubular thermal storage system and defines the numerical conventions used in this study. The second section provides a description of the symbols used and the assumptions made in the model. The third and fourth sections explain the discretization of the system into meshed elements and the transformation of the mesh coordinates. The fifth section focuses on the development of an evaluation algorithm for the thermal storage system. It presents the recursive process of the temperature field between elemental units over time and concludes with the design of size constraints for triangular fins and their geometric arrangement.

2.1. Physical model and computational domain

Figure 1: Phase change thermal energy storage tank

This paper aims to improve the structure of the heat exchange fin in the tank of the phase change heat storage system to further improve the heat transfer performance of the heat storage product. In a shell and tube heat storage tank, as shown in Fig.1, the tank is the core component of the heat storage system. The annular area is filled with a heat storage phase change material (PCMs) and a fin structure, The cross-section of the shell-and-tube thermal storage tank is shown in Fig.2. When PCM absorbs heat, the high-temperature working fluid circulates through internal pipes, storing and utilizing its waste heat. When the PCMs releases heat, the cryogenic working fluid circulates through internal pipes, absorbing and reusing the heat stored in the PCMs.

The research object is a small phase change heat storage tank, the inner radius of the tank is $0.02m$, the outer radius is $0.05m$, the thermal conductivity of the heat sink is 214 $W/(m \cdot K)$, the density of PCMs is $780kg/m3$, the thermal conductivity of the phase change material is $0.15W/(m \cdot K)$, and the temperature of the phase change is $333K$. The outside of the tube is adiabatic and the inside is filled with a working fluid at $373K$. The structure of heat exchange fin in the tank of phase change heat storage system will be designed to further improve the heat exchange performance of heat storage products.

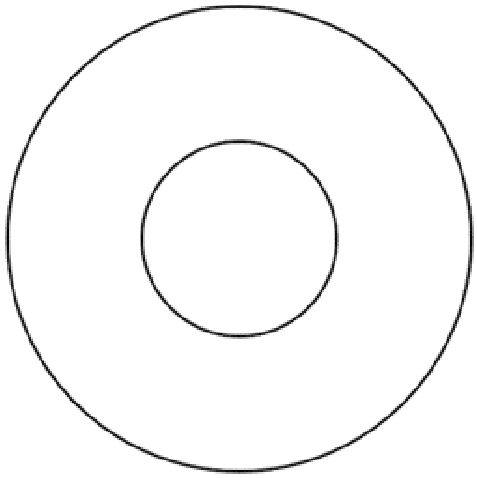

Figure 2: Phase change thermal energy storage tank

2.2. Symbol Description and Model Assumption

Table 1: Symbol Description

Symbol	Description
λ	Thermal conductivity
T	Temperature
t	Heat transfer time
n	Number of fins
Q_i	The quantity of heat(temperature increase iK)
S	Area of a fin
H	The height of the triangular fin
L	The base length of the triangular fin
C	The circumference of a fin
Eva	The evaluation value of fin performance
$triangular$	upright triangular fin
$un\_triangular$	Inverted triangular fin

In order to quantify the uncertainty in model and solution process, it is necessary to make some simplifying assumptions.

- Because the heat storage tank is a cylinder structure, and the length distribution of the cylinder is uniform. Therefore, our analysis of phase change heat storage tank is based on two-dimensional interface.

- The thermal conductivity of the fin is 214 times of PCMs, which is much larger than PCMs. Therefore, the heating time of the fin has little influence on the time for PCMs to reach the phase transition temperature, so it is ignored.

- It is assumed that PCMs is evenly distributed in the ring.

2.3. Analysis of heat transfer process without fins

Analyze and establish a mesh-based heat transfer model without considering the effects of fins. according to the heat conduction equation:

$$\lambda \Delta T = c\rho \frac{\partial T}{\partial t} \tag{1}$$

When all positions in the ring are satisfied $\partial T/\partial t = 0$, the mean temperature of all PCMs rose from room temperature ($293K$) to the transition temperature. But the specific heat capacity is unknown, and the two-dimensional temperature field is difficult to obtain from the heat conduction equation. So we design a new model that can replace the standard heat conduction equation without the specific heat capacity. And can reflect real-time temperature field. The termination condition is when all the PCMs temperatures in the ring space reach the phase transition temperature. According to the definition of thermal conductivity, that is, under the condition of stable heat transfer, the temperature difference between the two surfaces of a material 1 meter thick is the heat transferred within 1 hour. The thermal conductivity of the PCMs is 0.15 $W/(m \cdot K)$. It can be abstracted as PCMs gaining heat Q $0.15W$ by traveling 1 meter in 1 hour. But one meter is a big distance, and getting energy is not linear. Calculus tells us that the amount of energy gained by rising 1K over a very short distance and time must be stable.

Let the Δt=0.1s,ΔT=1K, because the thermal conductivity of the PCMs $\lambda = 0.15W/(m \cdot K)$, the distance required for the temperature rise of $1K$ within 0.1 seconds can be calculated as Δx=1/5400m. What's more, it is analyzed on a two-dimensional plane, so the unit distance in both the horizontal and vertical directions is set to 1/5400 meters. It forms a square grid. The radius of the outer circle is 0.05 meters, so 540×540 grids are needed to cover the entire interface.

According to the above, we set the heat conduction model as shown in Fig.3. The whole section is segmented by 540×540 grids, in the Δt=0.1s, the maximum propagation of Q_1 energy causes the adjacent grid to heat up $1K$.

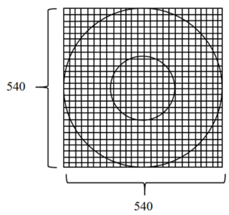

Figure 3: Grid section

2.4. The judgement of a small grid position

When the initial state is set as $t = 0$, the temperature field of the whole heat storage tank section should be established first. The temperature of the fin and inner circle space is $373K$, and the temperature of the remaining PCMs space is $293K$. The method of finite element grid section was used to build the model. So the problem can be transformed into judge the position of each grid and whether its position is in the PCMs region, the fin region or the inner circle region. Establish a coordinate system with the center of a circle as the origin as shown in the Fig.4. In order to facilitate the calculation of the grid position, the center point (x, y) of the grid is taken as the coordinate information of the grid. The grid number (i, j) starts from the lower left corner and increases upward and right respectively. The corresponding relationship between grid numbering and grid coordinates can be obtained as:

$$\begin{cases} x = (j - 270) * (1/5400) - (1/10800) \\ y = (i - 270) * (1/5400) - (1/10800) \end{cases} \tag{2}$$

In this way, information about the coordinates can be obtained, and then the region of the grid can be determined.That is, when $\sqrt{x^2 + y^2} \leq 0.05$, the grid is in the effective region (PCMs region); when $\sqrt{x^2 + y^2} \leq 0.02$, the grid is in the inner circle region.

For the judgment of rectangular fins area, the length of the rectangular fin is $0.018m$, the width is $0.006m$ and the θ when the number of fins are fixed, thus the equation of the center coordinate of the rectangle can be obtained:

$$\begin{cases} x_0 = (0.02 + 0.018/2) * sin(\theta) \\ y_0 = (0.02 + 0.018/2) * cos(\theta) \end{cases} \tag{3}$$

As long as the distance from the grid coordinate (x, y) to the vector (x_0, y_0) is less than half of the width of the rectangle and the projection distance of (x, y) to the vector (x_0, y_0) is less than half of the length, the grid is in the area of rectangular fins. The initial temperature field is shown in the Fig.5. Where red area represents the initial temperature of $293K$ in the PCMs region. The white in the middle indicates that the temperature is $373K$.

As can be seen from the Fig.6, If Area($\triangle ABC$)= Area($\triangle ABD$)+Area($\triangle BCD$)+Area($\triangle CDA$) is obtained, the grid can be judged to be in the triangular fin region. it can be judged whether the grid points are in the triangle fin by comparing the relationship between the area of $\triangle ABC$ and the sum of the areas of $\triangle ABD$,$\triangle BCD$ and $\triangle CDA$. The temperature field in the initial state is shown as the Fig.7. where red indicates the initial temperature of the PCMs region is $293K$, and white in the middle indicates the temperature of the region is $373K$.

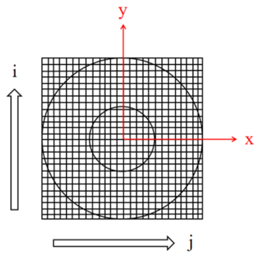

Figure 4: Grid and section coordinate system

Figure 5: Initial temperature field (n=4)

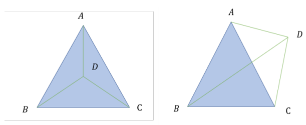

Figure 6: riangular region

Figure 7: Initial temperature field (H=0.013m n=8)

2.5. Model establishment

2.5.1. Performance indicators for the heat storage tank

when the fin size and shape was given, with the increase of the number of fins, the total heat transfer time decreases as a whole. However, the comprehensive evaluation of heat transfer rate of heat storage tank is not only one factor of time, maximum energy storage capacity is also an important factor. The maximum energy storage of the heat storage tank is linearly related to the area of PCMs in the section. The value of the heat storage tank's heat transfer performance evaluation is denoted as E. E is inversely proportional to the total time t_{total}, and is proportional to the area of PCMs in the section. Naturally, it is inversely proportional to the area occupied by the fin in the section. Heat transfer performance evaluation values are defined as:

$$Eva = \frac{1}{t_{total} * S * n} \tag{4}$$

Although the product of t and $s * n$ can reflect the performance of the heat storage tank to some extent, this indicator has too one-sided problems. When the value of $s * n$ is large and the value of t is small, their product may be small, resulting in a lower value of E, which is not in line with reality. To solve the one-sidedness of the equation(4), we introduce $t + s * n$, a new composite metric that combines time and area. When one of the items is smaller, the overall result does not fluctuate greatly. Therefore, we redefine the rating value as:

$$Eva = \frac{1}{t_{total} * S * n + t_{total} + S * n} \tag{5}$$

In order to harmonize the units of measurement for fin area and heat transfer time, and to ensure that their range of values is consistent, we introduce the following definition: the proportion of the area of the fin in the space of the phase change material is expressed as $S^{'}$, and the ratio of the total heat transfer time of the fin to the heat transfer time without the fin is expressed as $t^{'}$. With such a definition, they will all remain between 0 and 1. Therefore, we can conclude that the final fin heat transfer performance evaluation value is:

$$Eva = \frac{1}{t' * S' + t' + S'} \tag{6}$$

2.5.2. Heat transfer model

With the initial temperature field in the Fig.5 above, we can simulate the change of temperature field over time. The premise of temperature propagation in the temperature field is that there is a temperature difference, and in time Δt , the energy from the grid with a relatively high temperature only diffuses outward to the adjacent grid with a low temperature. Because of the law of conservation of energy, this energy is not greater than Q_1.The energy diffusion form of high energy grid was analyzed in the following.

As shown in the Fig.8, the energy of grid 4 is assumed to be much higher than that of grid 0,1,2,3. So in time Δt, grid 4 diffused the energy Q_1 to other neighboring low temperature grids. In this way, grid 0,1,2,3 will on average gain a quarter of the energy of grid 4, which is denoted as $Q_{0.25}$, in other words, temperature increase 0.25K. Then, in the next adjacent time, the energy of grid 0,1,2,3 diffusing outward to the adjacent low temperature grid is only $Q_{0.25}$, except to reach the phase transition temperature, the energy diffusing is Q_1.According to the energy diffusion model above, set the number of grid 4 as (i, j) , and the temperature difference between grid 0,1,2,3 and adjacent grids is denoted as T_0, T_1, T_2, T_3. Because energy can only be transferred from the hot side to the cold side, it can only be transmitted when the temperature difference is greater than 0. In combination with practical application, a grid can only have two adjacent grids at most, so there are altogether 10 diffusion modes.

(1) When the temperature difference of only one side is greater than 0, for example, $T_0 > 0$, $T_1 \leq 0$, $T_2 \leq 0$,$T_3 \leq 0$, the energy obtained by the grid $(i, j-1)$ is the minimum value between the energy obtained of grid (i, j) in the last Δt and the energy Q_{T_0}. Because the phase change temperature is 333K, the maximum temperature cannot exceed 333K, the expression is:

$$b_{(i,j-1)} = min\left(min\left(c_{(i,j)}, T_0\right) + b_{(i,j-1)}, 333\right) \tag{7}$$

where $b_{(i,j-1)}$ is the temperature of grid (i, j) in the current time period, and $c_{(i,j)}$ is the temperature difference of grid(i, j) in the last Δt.The same is true for other cases where the temperature difference of one side is greater than 0.

(2) When the temperature difference between two sides is greater than 0, for example, $T_0 > 0$, $T_1 > 0$, $T_2 \leq 0$,$T_3 \leq 0$. At this time, we need to analyze 4 cases, but due to the limit of boundary temperature, the final temperature cannot exceed the phase change temperature ($333K$).

- When the $T_0 \geq c_{(i,j)}/2$ and $T_1 \geq c_{(i,j)}/2$, the temperature of two adjacent grids also rise $c_{(i,j)}/2$.

$$\begin{cases} b_{(i,j-1)} = min\left(\frac{c_{(i,j)}}{2} + b_{(i,j-1)}, 333\right) \\ b_{(i+1,j)} = min\left(\frac{c_{(i,j)}}{2} + b_{(i+1,j)}, 333\right) \end{cases} \tag{8}$$

- When the $T_0 < c_{(i,j)}/2$ and $T_1 < c_{(i,j)}/2$, the temperature of two adjacent grids rise respectively T_0,T_1.

$$\begin{cases} b_{(i,j-1)} = min\left(T_0 + b_{(i,j-1)}, 333\right) \\ b_{(i+1,j)} = min\left(T_1 + b_{(i+1,j)}, 333\right) \end{cases} \tag{9}$$

- Only when the $T_0 < c_{(i,j)}/2$, the temperature of grid $(i, j-1)$ rise T_0, while the rising value of temperature of grid $(i+1, j)$ is the minimum value between $c_{(i,j)} - T_0$ and T_1.

$$\begin{cases} b_{(i,j-1)} = min\left(T_0 + b_{(i,j-1)}, 333\right) \\ b_{(i+1,j)} = min\left(min\left(c_{(i,j)} - T_0, T_1\right) + b_{(i+1,j)}, 333\right) \end{cases} \tag{10}$$

- Only when the $T_1 < c_{(i,j)}/2$, it is same with the above case.

$$\begin{cases} b_{(i+1,j)} = min\left(T_1 + b_{(i+1,j)}, 333\right) \\ b_{(i,j-1)} = min\left(min\left(c_{(i,j)} - T_1, T_0\right) + b_{(i,j-1)}, 333\right) \end{cases} \tag{11}$$

The other 5 kinds of recursion relationship of bilateral temperature transfer can be obtained in the same way.

In summary, analyzed the recursive relationship of temperature field over time,the stopping condition of the recursive relationship is that all the grid temperatures in the PCMs region rise to $333K$.

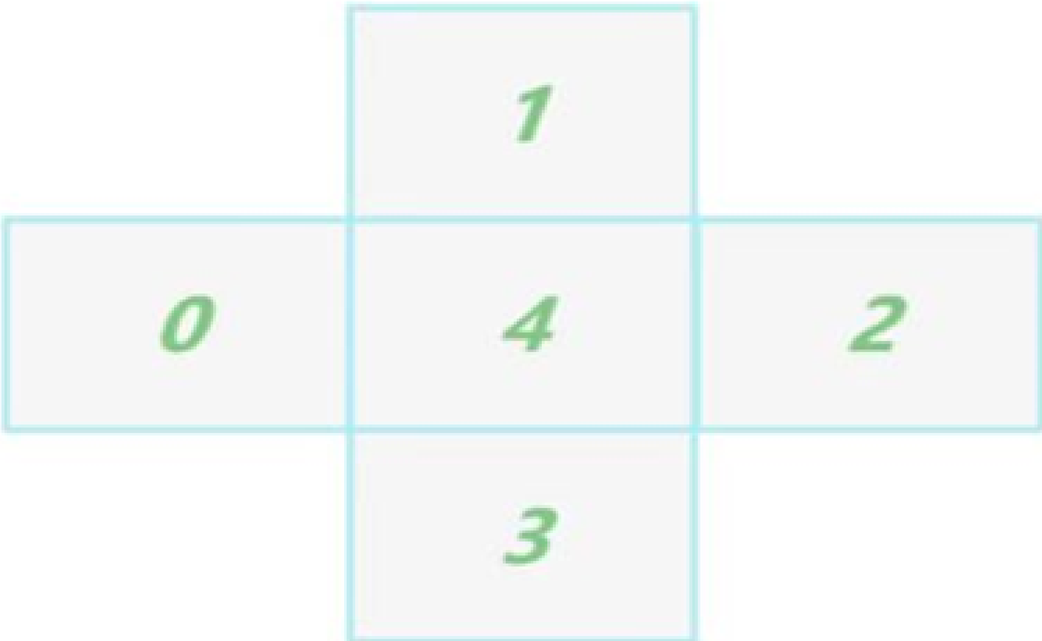

Figure 8: Heat transfer of grid

2.5.3. Constraints of triangular fin

the design model of fin size should not only consider the influence of time on heat transfer performance of heat storage tank, but also consider the influence of maximum energy storage value of heat storage tank. According to the definition of heat flow, the maximum energy that the fin can store is denoted Q and defined $Q = \lambda * S * \Delta T$. According to Fig.8 , if grid 4 is to transfer energy Q_1 to adjacent low-temperature grids, the energy in grid 4 should be at least Q_4. The grid adjacent to each fin should be able to obtain the energy Q_1 in the initial state, and the total energy of the grid adjacent to each fin is denoted as Q_c. In this case, the energy transmission must satisfy the inequality relation $Q \geq C \quad (\lambda * S * \Delta T \geq C)$. In order to facilitate the establishment of the following model, given the base length of the triangular fin as L and the height as H. According to the definition of E, in order to achieve the optimal value of the evaluation value E, the area $S * n$ of the fins in the section should be the minimum value. So make the equation that is $C = \lambda * S * \Delta T$. Given $\lambda_{fin} = 214, \Delta T = 4$, the area and circumference of the fins are respectively:

$$S = H * L * 1/2 \tag{12}$$

$$C = 2\sqrt{H^{2+}\frac{L^2}{4}} + L \tag{13}$$

he relation between H and L can be obtained as:

$$L = \frac{H}{\sqrt{(428 * H - 0.5)^2 - 0.25}} \tag{14}$$

where $(428 * H - 0.5)^2 - 0.25 > 0$.

It can be seen that the high H of triangular fins is a variable affecting the total heat transfer time and the maximum number n of fins. In order to achieve better experimental results, we sampled H with a step size of $0.001m$, and obtained from $(428 * H - 0.5)^2 - 0.25 > 0$ the solvable minimum value is $0.003m$, and the maximum value H is the radius difference between the outer circle and the inner circle is $0.03m$. the Fig.9 shows parts of the different values of H and corresponding values of n.

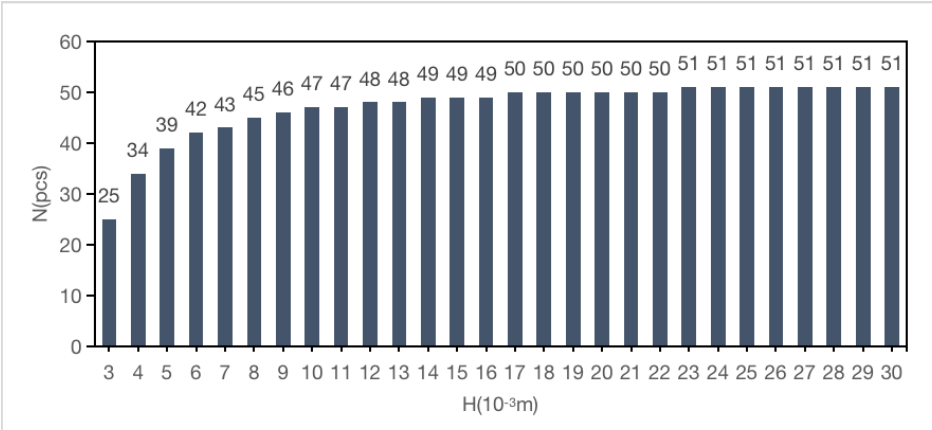

Figure 9: Relationship between fin height and maximum number of fins that can be arranged

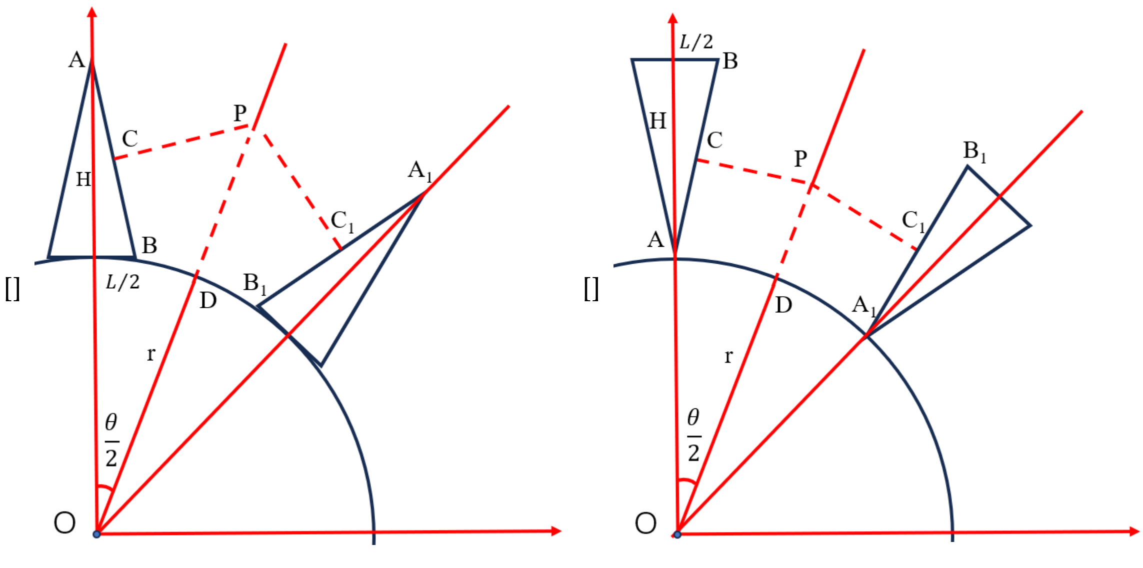

Figure 10: Distance field

2.5.4. Distance field of triangular fins

According to the definition of thermal conductivity, the farther away from the heat source in continuous space, the longer it takes to raise the same temperature. Therefore, the heat conduction time has a direct relationship with the distance between the two fins and the heat conduction distance of the inner arc between the fins.

Assume a simple range field model. Make three normal vectors intersect at the midpoint of the two fins and the section where the midpoint of a small arc is located. In this case, the distance field of the section is the sum of the distance of the intersection point to the three surfaces. In upright triangular fins, as shown in Fig.**??**,The normals CP and C_1P correspond to the midpoints of two adjacent fins, while DP represents the normal at the midpoint of $\overset{\frown}{BB_1}$. These normals intersect at point P.The distance field is then defined as follows:

$$Len = CP + C_1P + DP = CP + C_1P + OP - r \tag{15}$$

Similarly, the distance field of inverted triangular fins shown in Fig.**??** is defined in the same way as in Equation(15). Therefore, the distance field for the two types of fins can be obtained as follows:

$$Len_{triangular} = \frac{r + \frac{H}{2} - \frac{L^2}{8H}}{tan\frac{\theta}{2} - \frac{L}{2H}} \bullet \frac{1}{sin\frac{\theta}{2}} + CP + C_1P - r \tag{16}$$

$$Len_{un-triangular} = \frac{r + \frac{H}{2} + \frac{L^2}{8H}}{tan\frac{\theta}{2} + \frac{L}{2H}} \bullet \frac{1}{sin\frac{\theta}{2}} + CP + C_1P - r \tag{17}$$

If the two types of triangular fins have the same size and angle, then CP and C_1P will have the same length. To compare the distance fields of the two types of fins, we only need to compare the length of OP. It can be calculated that $Len_{un\_triangular}$ less than $Len_{triangular}$. Therefore, based on the inference from the distance field, the geometric shape of the new type of fin in this study is designed as an inverted triangle. The temperature field is initialized, and the initial state of the obtained temperature field is shown in Fig.11.

Since the model is an inverted triangle, the maximum value of H occurs when it intersects with the outer circle. At this point, the maximum value of H is approximately $0.029m$, while the minimum value of H remains at $0.003m$. In addition, the maximum number of fins that can be filled in the tank will also change. The change is shown in Fig.12.

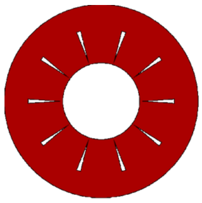

Figure 11: Initial temperature field (H=0.018m n=10)

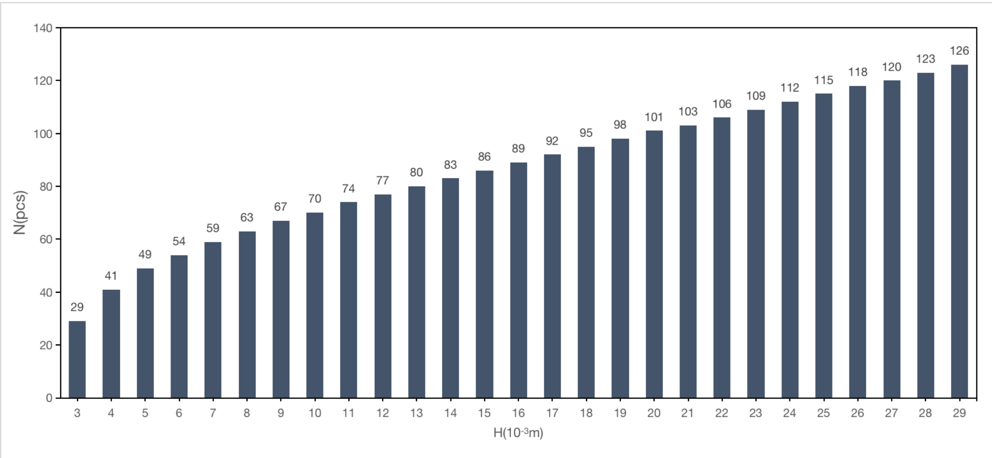

Figure 12: The relationship between the height of inverted triangular fins and the maximum number of fins that can be arranged

3. Validation of numerical simulation

3.1. Validation of time step and mesh number

In section 2.3, the relationship between the time step and the number of grid cells was derived based on the thermal conductivity. When the time step is 0.1s, the number of grid cells is 540×540. When the time step is 0.05s, the number of grid cells is 1080×1080. When the time step is 0.025s, the number of grid cells is 2160×2160. To eliminate the influence of the time step and grid size on the simulation results, a comparison test was conducted using these three different time steps. The experiment involved rectangular fins with different numbers, and the relationship between the total heat transfer time and the number of fins at different time steps (corresponding to different grid sizes) is shown in Fig.13. The average error of the calculated results is within 10s. It can be concluded that further refinement of the grid size or reduction of the time step will not significantly affect the calculation results. A time step of 0.1s (with a grid size of 540×540) is sufficient to achieve the required accuracy.

Furthermore, using seven rectangular fins as carriers further verified the effect of the time step on the heat transfer process. The focus of the calculation was on the proportion of the phase change area of the PCM to the total area of the PCM in the same period of time under different time steps. As shown in Fig.14, the average error of the phase change area of the PCM at the same time point under the three time steps (grid numbers) is within 1%. Fig.16 shows the temperature field under different time steps. To increase the distinguishability of the temperature field, the fins and the high-temperature working fluid in the inner ring are marked in yellow, and the temperature inside the annular ring corresponds to the temperature indicated by the color bar. In summary, the heat transfer process has little dependence on the time step.

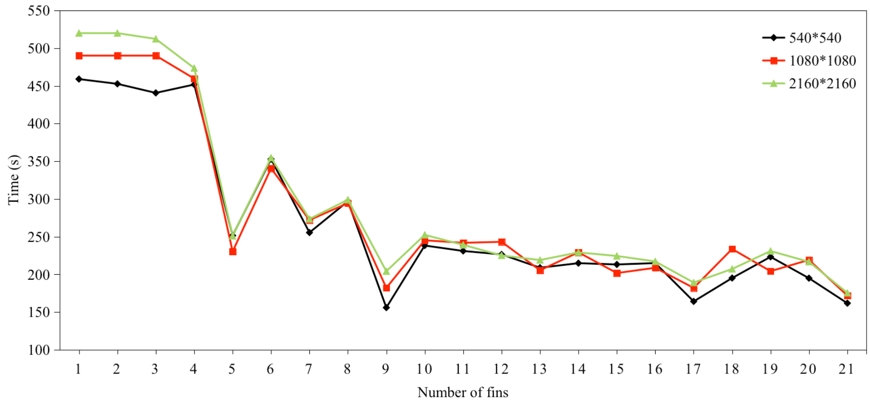

Figure 13: The duration of heat transfer

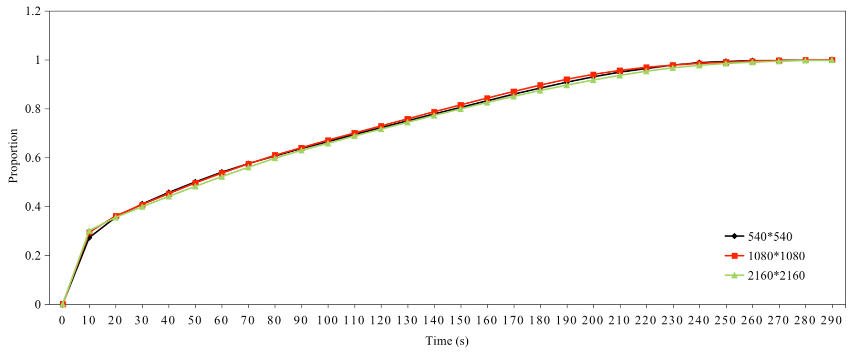

Figure 14: The proportion of phase change area

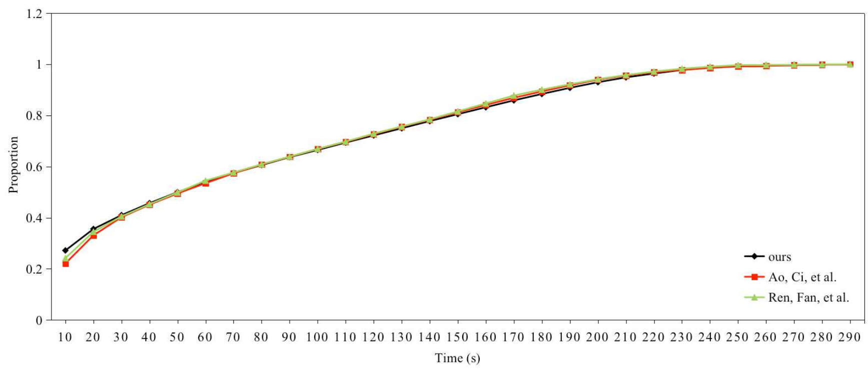

Figure 15: comparison of heat transfer simulations

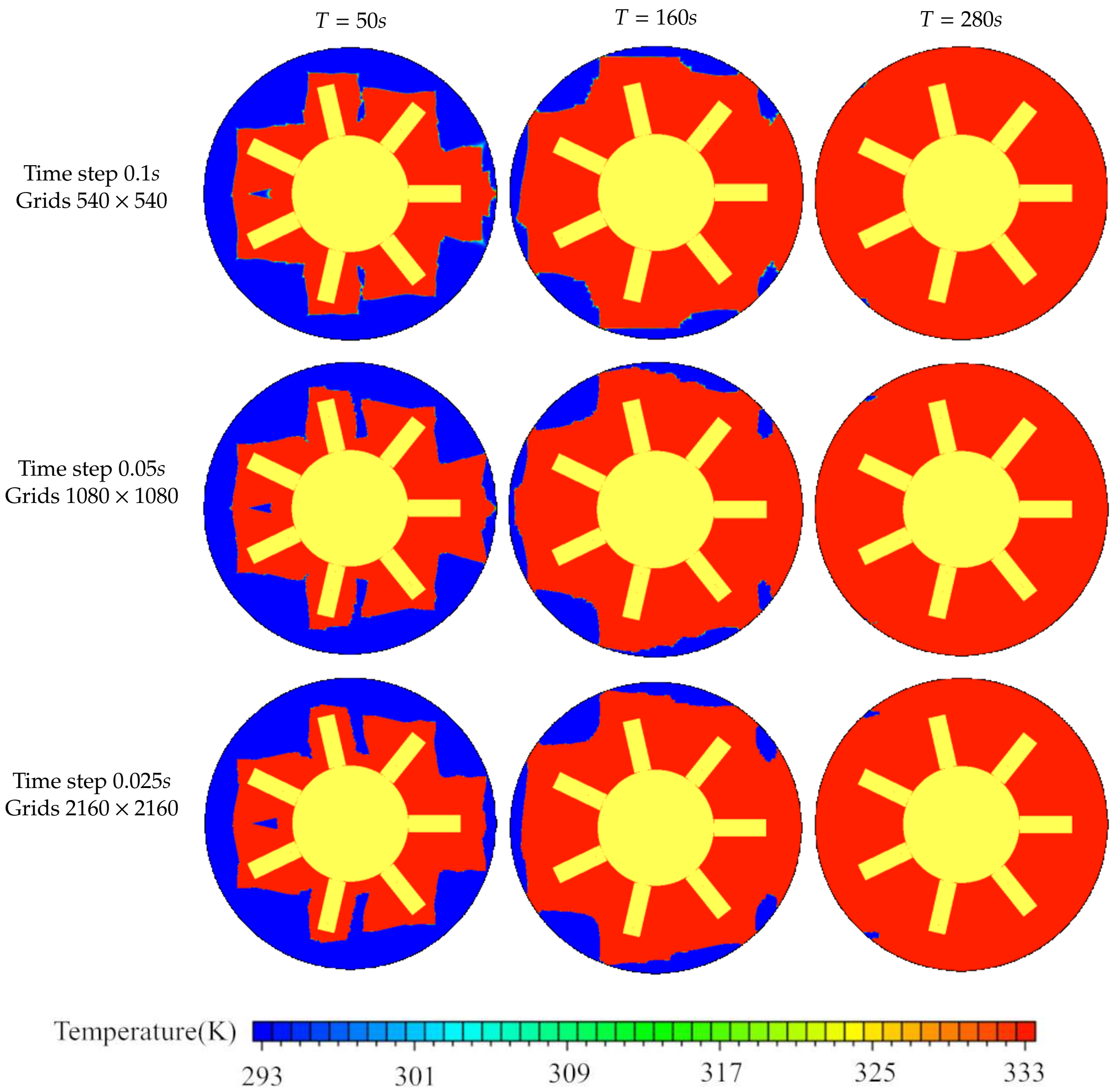

Figure 16: Temperature field

3.2. Validation of heat transfer model

Under the experimental conditions of a time step of 0.1s and a grid size of 540×540, using seven rectangular fins as carriers, the proportion of the PCM phase change area to the total PCM area during the same period of time was calculated under different time steps. The numerical results obtained in this study were compared with the calculation results of the algorithms in references [3] and [20], and the line chart is shown in Fig.15, where the horizontal axis represents the time point and the vertical axis represents the proportion of the PCM phase change area. The maximum error between the heat transfer model used in this study and other research methods is no more than 7%, and the average error is less than 2%. The movement of PCM phase change during the heat storage process was accurately predicted, which verifies the reliability of the numerical simulation algorithm proposed in this study.

4. Results and discussion

In this chapter, the geometry, size, and number of fins are studied, and we will analyze and synthesize the results of the experiments on fins with different geometries in four sections.

4.1. Rectangular fins

The dimensions of the rectangular fins are set to fixed values (H=0.018m, L=0.006m). This section will show the effect of different rectangular fin numbers on experimental results and determine the optimal value.

Based on the size of the rectangular fins, we can calculate the maximum number of fins that can be accommodated within the ring to be 20. Based on the heat transfer model in subsection 2.5.3, we calculate the heat transfer time at different fin numbers. The Fig.21 shows the PCMs temperature field with different number of fins at different time periods. In addition, we plotted heat transfer time curves for different fin numbers, as shown in Fig.17. In the following analysis, we calculate the evaluation index *Eva* according to the comprehensive evaluation method of the fins in subsection 2.5.1, and plot the *Eva* curve under different fin numbers, as shown in the Fig.18, The higher the *Eva* value in the line chart, the better the heat transfer performance corresponding to the number of fins.

Comparing the time map, it is not difficult to find that when n=8, the heat transfer time is the smallest, and in the *Eva* diagram, when n=8, the *Eva* value is also the highest, so when the rectangular fin size must be, select 8 fins evenly distributed in the ring as the best choice. The optimal layout of rectangular fins with fixed sizes is shown in Fig.19.

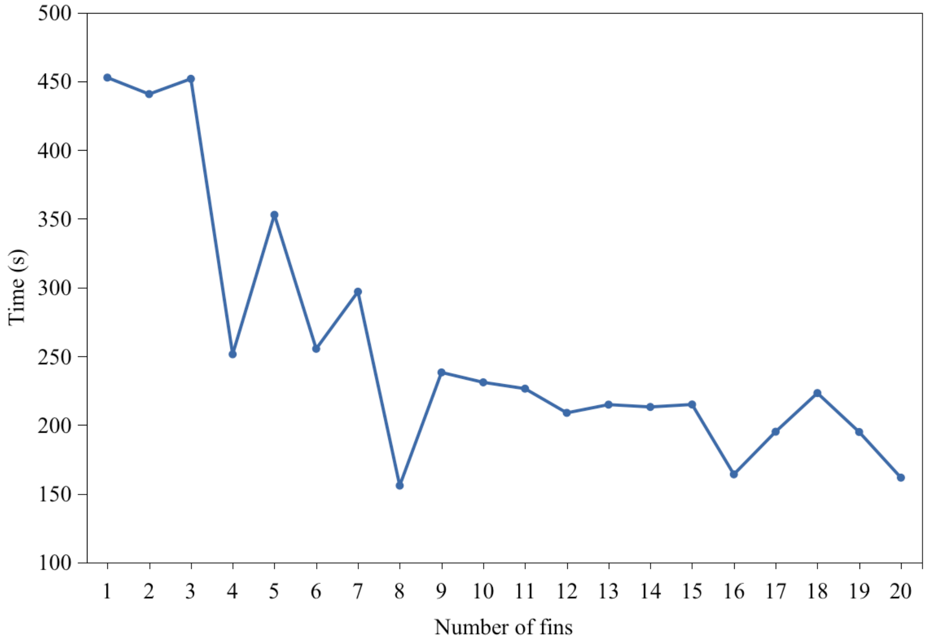

Figure 17: The duration of heat transfer for rectangular fins

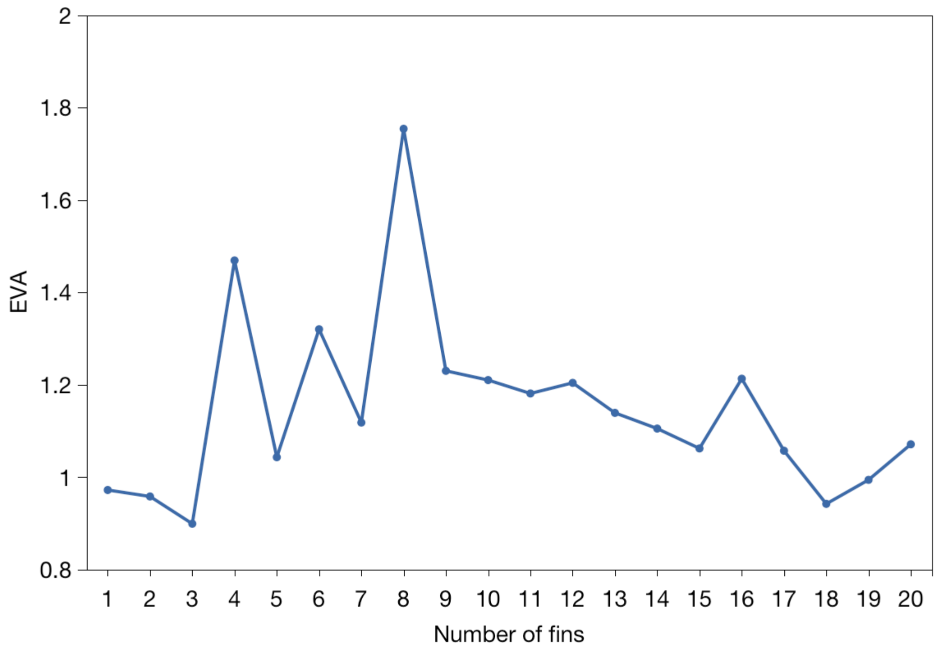

Figure 18: Performance evaluation of rectangular fins

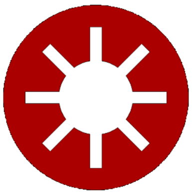

Figure 19: The optimal layout of rectangular fins

4.2. upright triangular fins

For upright triangular fins, with a height range of $H \in [0.003, 0.03]$, a height sampling step of $0.001m$ is used to calculate the heat transfer performance of 28 fins with different heights. To improve efficiency, a coarse sampling of H can be conducted first, followed by a fine sampling in the area with the optimal *Eva* value. Specifically, a larger step size is used to sample the height values, the height value with the maximum overall *Eva* value is found, and then a fine sampling with a step size of $0.001m$ around the maximum *Eva* value is performed to obtain the vertex with the maximum *Eva* value, corresponding to a unique fin size and number. The experimental steps and results of coarse and fine sampling are presented below.

For the coarse sampling, assuming a step size of $0.006m$ for the height of the fins, the discrete height points sampled are H=$0.003m$, H=$0.009m$, H=$0.015m$, H=$0.021m$, and H=$0.027m$. First, according to the algorithm in section 2.5.3, a unique L and a range of fin arrangements can be obtained for each height H. Then, using the heat transfer model in section 2.5.2, the heat transfer time under different heights and fin numbers can be calculated. Finally, the performance evaluation method in Equation(6) is used to calculate the *Eva* value under different heights and fin numbers. The experimental results are shown in Fig.22 and Fig.23, which respectively demonstrate the heat transfer time and *Eva* value under different heights and fin numbers. A higher *Eva* value indicates better fin performance. Therefore, according to the experimental results, the performance of upright triangular fins improves as the height increases. Specifically, during the coarse sampling, the optimal heat transfer performance is achieved when H=$0.027m$. For the fine sampling, assuming a step size of $0.001m$ for the height, the discrete height points around H=$0.027m$ with the best heat transfer performance are sampled, including H=$0.025m$, H=$0.026m$, H=$0.027m$, H=$0.028m$, H=$0.029m$, and H=$0.03m$. The experimental steps are the same as the coarse sampling, and the experimental results are shown in Fig.24 and Fig.25, which respectively demonstrate the heat transfer time and *Eva* value under different heights and fin numbers.

Based on the experimental analysis, it was found that when H=$0.03m$ and the number of fins n=16, the maximum *Eva* value achieved was 3.179. Fig.27 visualizes the temperature field of different upright triangular fins at different time intervals. The optimal parameters for the heat transfer performance of upright triangular fins are Height: H=$0.03m$, Length: L=$0.0024m$, and the fin angle: $\theta = \pi/8$. The layout with the best performance for upright triangular fins is shown in Fig.20.

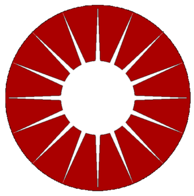

Figure 20: Optimal arrangement of upright triangular fins

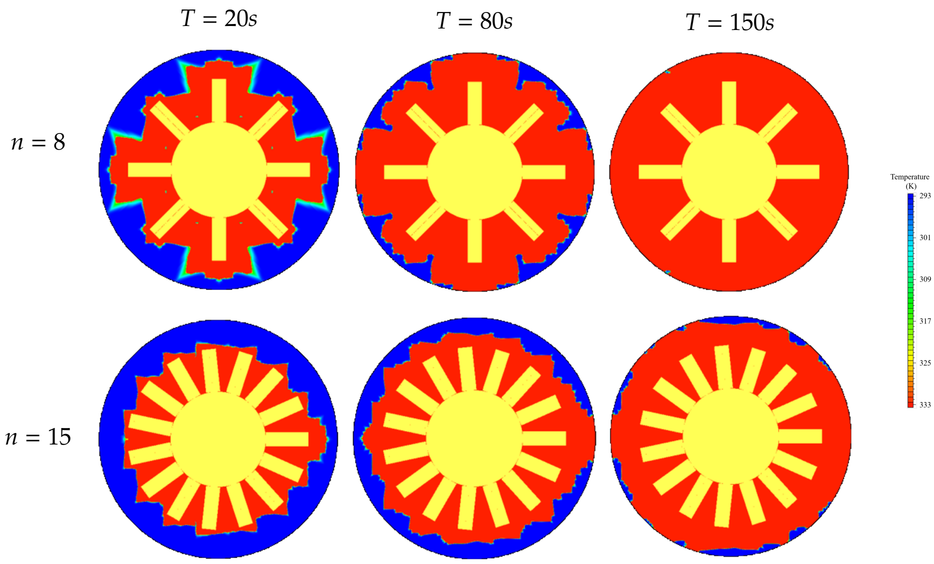

Figure 21: Temperature field of rectangular fins

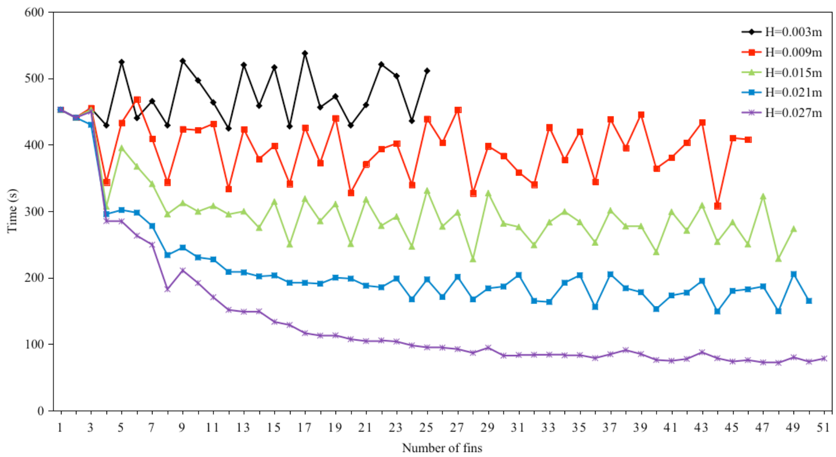

Figure 22: Heat transfer duration of upright triangular fins with rough sampling

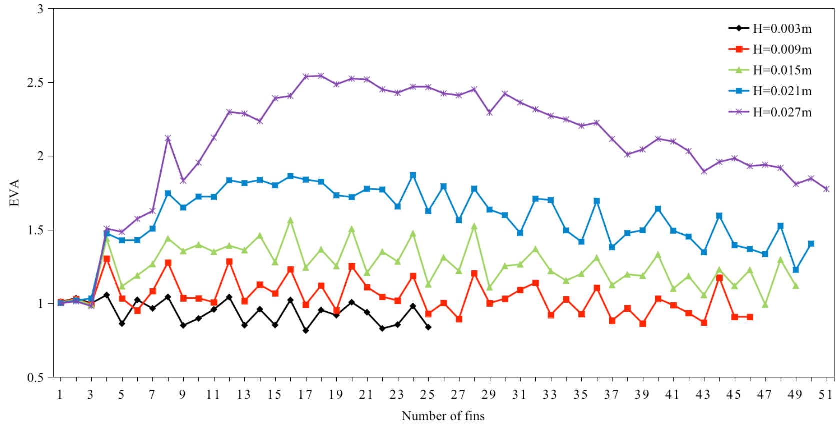

Figure 23: Performance evaluation of upright triangular fins with coarse sampling

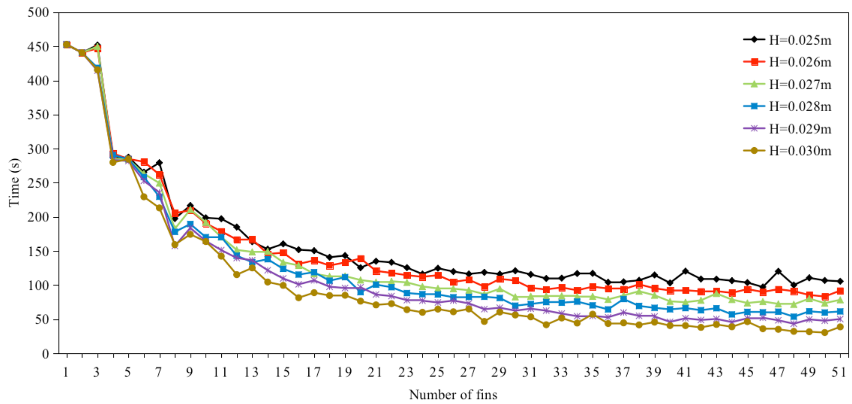

Figure 24: Heat transfer duration of upright triangular fins with fine sampling

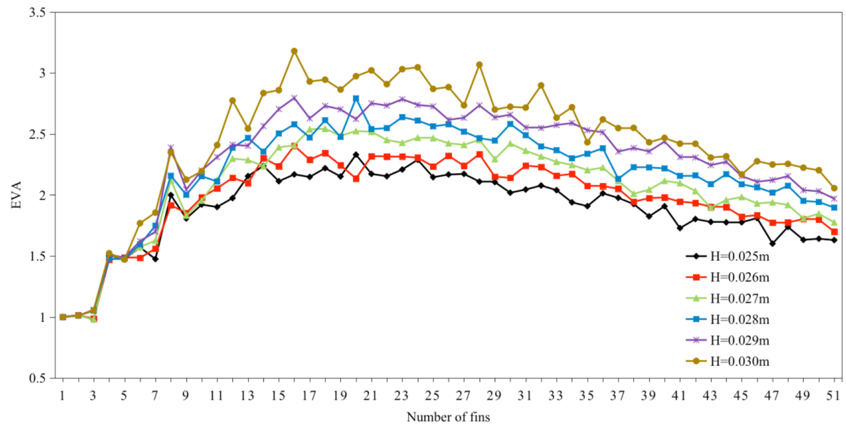

Figure 25: Performance evaluation of upright triangular fins with fine sampling

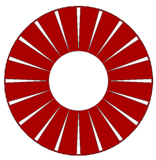

Figure 26: Performance evaluation of Inverted triangular fins with fine sampling

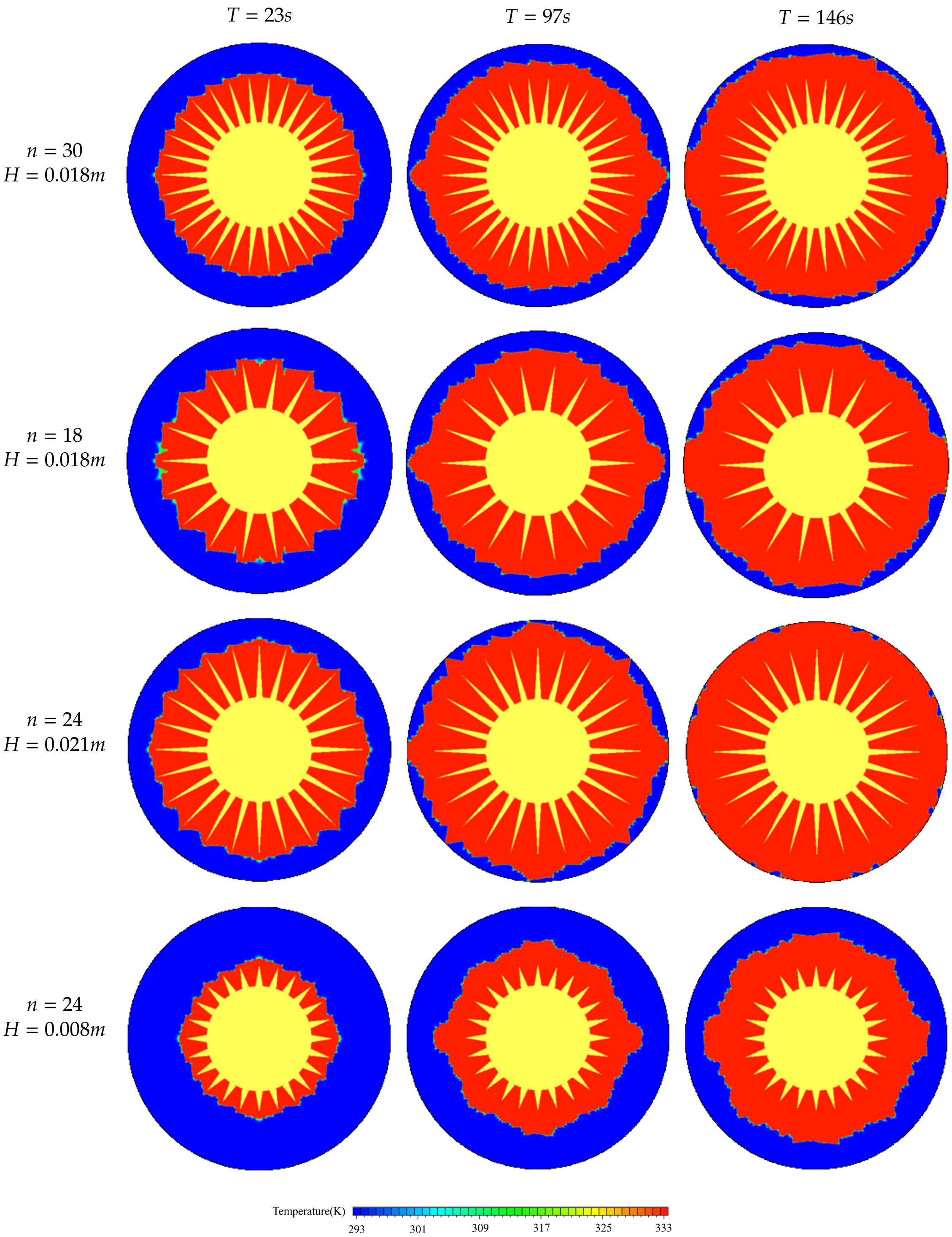

Figure 27: Temperature field of upright triangular fins

4.3. Inverted triangular fins

For inverted triangular fins with $H \in [0.003, 0.029]$, a height sampling step of $0.001m$ is required to calculate 27 fins with different heights. To improve experimental efficiency, a coarse sampling of H can be conducted first, followed by a fine sampling in the area with the optimal *Eva* value. Specifically, a larger step size is used to sample the height values, the height value with the maximum overall *Eva* value is found, and then a fine sampling with a step size of $0.001m$ around the maximum *Eva* value is performed to obtain the vertex with the maximum *Eva* value, corresponding to a unique fin size and number. The experimental steps and results of coarse and fine sampling are presented below.

In the coarse sampling, assuming a step size of $0.006m$ for the height of the inverted triangular fins, the discrete height points sampled are H=0.003m, H=0.009m, H=0.015 m, H=0.021m,and H=0.027m. Firstly, according to the algorithm in section 2.5.3, a unique L and a range of fin arrangements can be obtained for each height H. Then, using the heat transfer model in section 2.5.2, the heat transfer time under different heights and fin numbers can be calculated. Finally, the performance evaluation method in Equation(6) is used to calculate the *Eva* value under different heights and fin numbers. The experimental results are shown in Fig.28 and Fig.29, which respectively demonstrate the heat transfer time and *Eva* value under different heights and fin numbers. A higher *Eva* value indicates better fin performance. Therefore, according to the experimental results, the performance of inverted triangular fins improves as the height increases. Specifically, during the coarse sampling, the optimal heat transfer performance is achieved when H=0.027m. For the fine sampling, assuming a step size of 0.001m for the height, the discrete height points around H=0.027m with the best heat transfer performance are sampled, including H=0.025m, H=0.026m, H=0.027m, H=0.028m, and H=0.029m. The experimental steps are the same as the coarse sampling, and the experimental results are shown in Fig.30 and Fig.31, which respectively demonstrate the heat transfer time and *Eva* value under different heights and fin numbers.

Based on the experimental analysis, it was found that when H=0.029m and the number of fins n=20, the maximum Eva value achieved was 3.572. Fig.32 visualizes the temperature field of different inverted triangular fins at different time intervals. The optimal parameters for the heat transfer performance of inverted triangular fins are: Height:H=0.029m, Length: L=0.0024m, and the fin angle: $\theta = \pi/8$. The layout with the best performance for inverted triangular fins is shown in Fig.26.

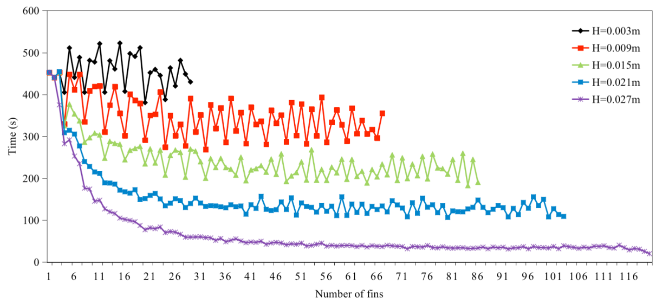

Figure 28: Heat transfer duration of Inverted triangular fins with rough sampling

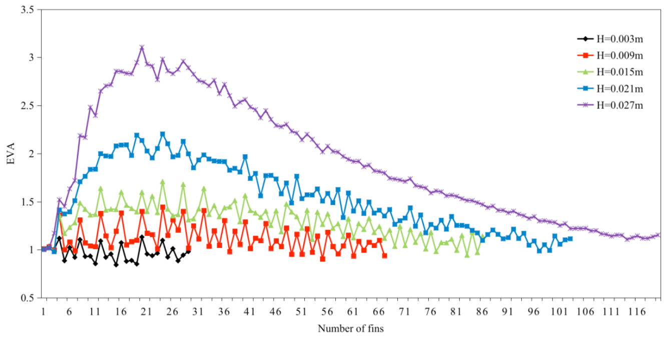

Figure 29: Performance evaluation of Inverted triangular fins with coarse sampling

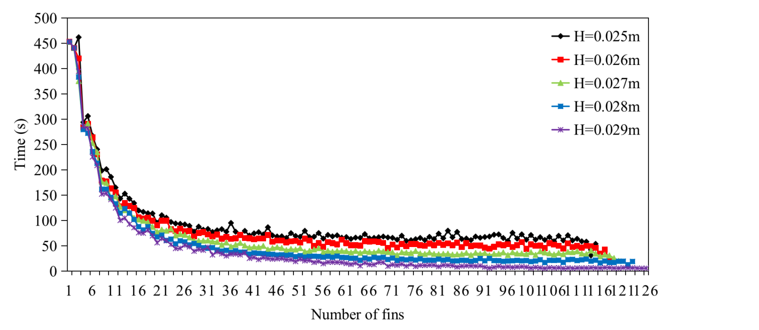

Figure 30: Heat transfer duration of Inverted triangular fins with fine sampling

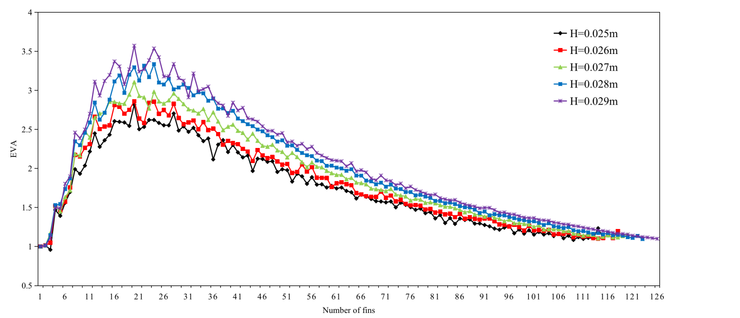

Figure 31: Performance evaluation of Inverted triangular fins with fine sampling

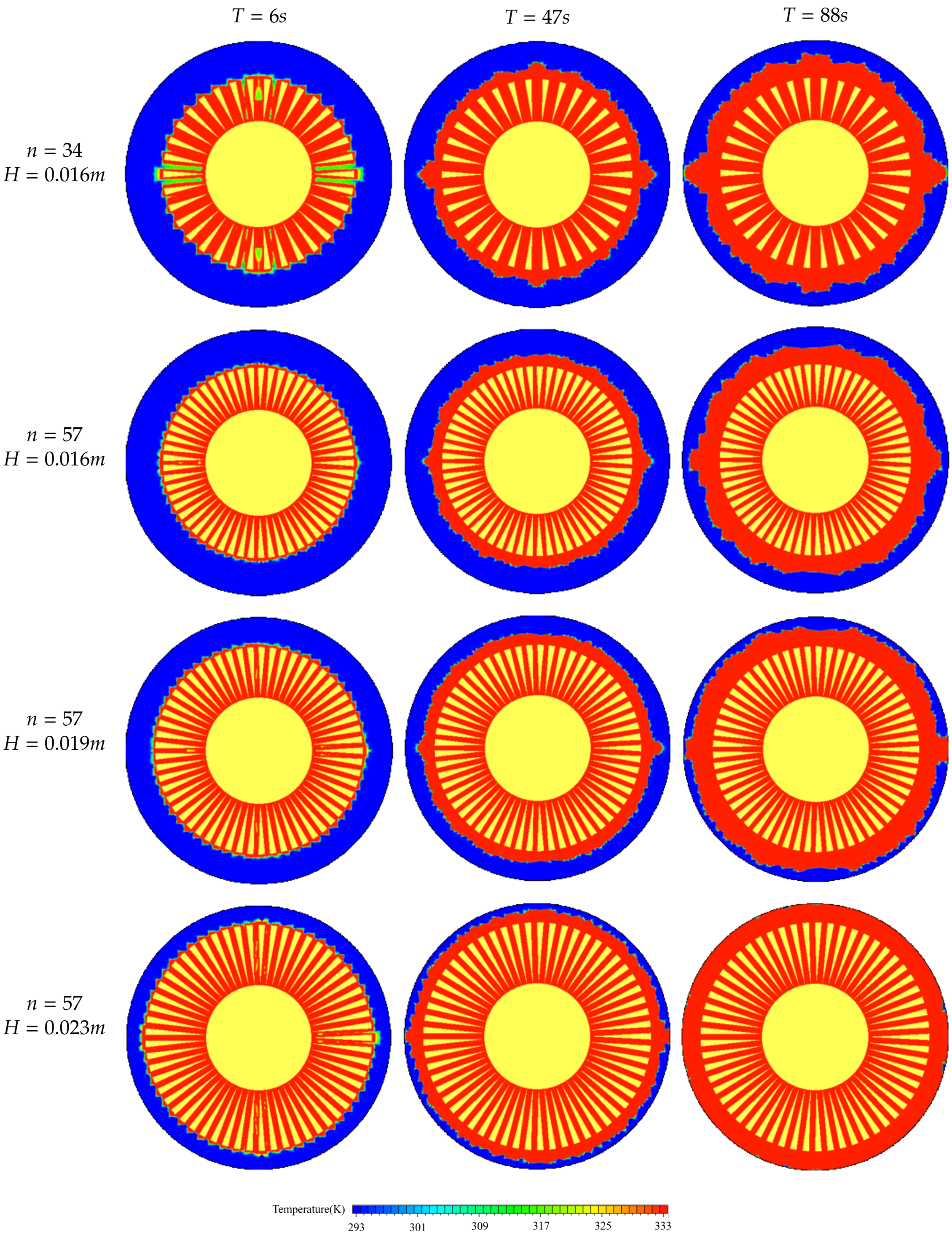

Figure 32: Performance evaluation of Inverted triangular fins with fine sampling

[Comparison of heat transfer time] 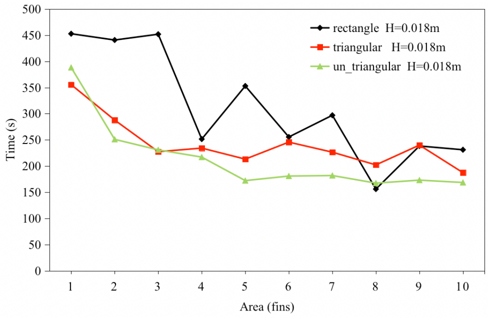

[Comparison of

performance evaluation] 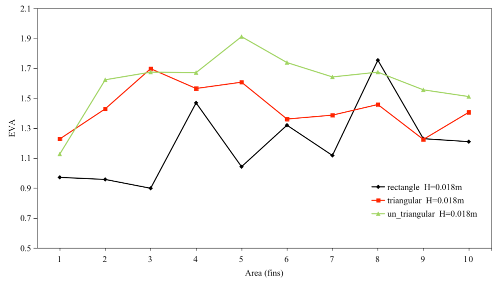

[Comparison of heat transfer

time] 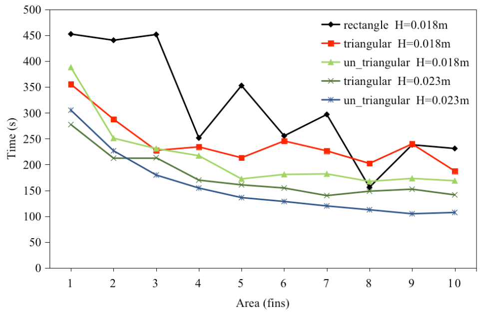

[Comparison of performance evaluation]

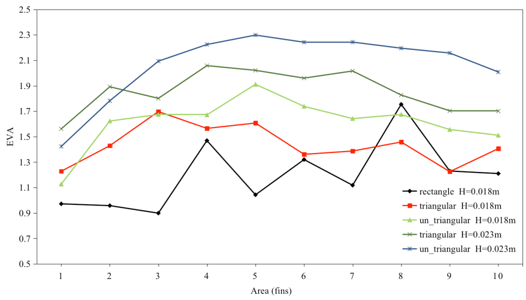

Figure 33: Comparison of performance evaluation and heat transfer time

4.4. Comprehensive comparison

This chapter discusses heat transfer between rectangular fins at different numbers and regular and inverted triangle fins in different sizes and quantities, and analyzes the optimal fin size and number. The following subsections will consider these three fins and compare their geometries to assess their advantages and disadvantages.

To improve the reliability of the experiment, we chose to compare *Eva* values at the same fin area. In addition, the height of the rectangular fin is set to 0.018*m*, and the height of the triangular fin is set to H=0.018*m*. According to the Equation(14), we can get L=0.0025*m*. In the case of the same area, there is the following relationship between the number of triangular fins n_1 and the number of rectangular finsn_0: $n_0 * 0.018 * 0.006 = n_1 * 0.018 * 0.0025 * 0.5$. The number of rectangular fins ranges from 1 to 20. Since the maximum number of permutations of positive triangular fins is 51, which corresponds to an area of 10 for the number of rectangular fins, the value range of the number of rectangular fins is set from 1 to 10, and the number of triangular fins is determined accordingly. Under the same height and area conditions, the heat transfer time and *Eva* performance index of fins of different geometries were compared, and the results were shown in the Fig.**??** and Fig.**??**, The horizontal axis represents the number of rectangular fins, which represents the area occupied by different numbers of rectangular fins. The vertical axis represents the heat transfer time and *Eva* value. According to the trend of the overall *Eva* value in the graph, the performance of inverted triangular fins is better than that of upright triangular fins, and the performance of upright triangular fins is better than that of rectangular fins.

For the purpose of investigating the correlation between the heat transfer performance of triangular fins and the fin size, particularly the impact of the height, the height of the triangular fins was chosen to be H=0.023*m* while keeping the principle of consistent surface area. A comparative experiment was conducted with the same parameters as the previous one.The experimental results are shown in the Fig.**??** and Fig.**??**, Fig.34 shows the temperature field of the three types of fins with the same area when the number of rectangular fins is 8, while Fig.35 shows the same condition when the number of rectangular fins is 10. According to the overall trend of Eva values in the graph, the order of fin performance from best to worst is: *a*) Inverted triangular fins with a height of 0.023*m*, *b*) upright triangular fins with a height of 0.023*m*, *c*) Inverted triangular fins with a height of 0.018*m*, *d*) upright triangular fins with a height of 0.018m,*e*) Rectangular fins.

Combining the chart and experimental results, we can draw the following conclusions:

- Fins with triangular geometry are superior to rectangular fins, and fins with inverted triangle geometry are superior to upright triangle fins, which verifies the theory of triangular fin distance field.
- Under the condition that the total area of the fin is the same, the larger the height(H) of the fin, the better the heat transfer performance of the fin.
- Too many or too few fins will lead to a decrease in heat transfer performance. Therefore, in general, it is desirable to choose the median value of the number of fins. Under the condition that the heat transfer time and the total area of the fins are constrained, the higher *Eva* value corresponds to the ideal number of fins.

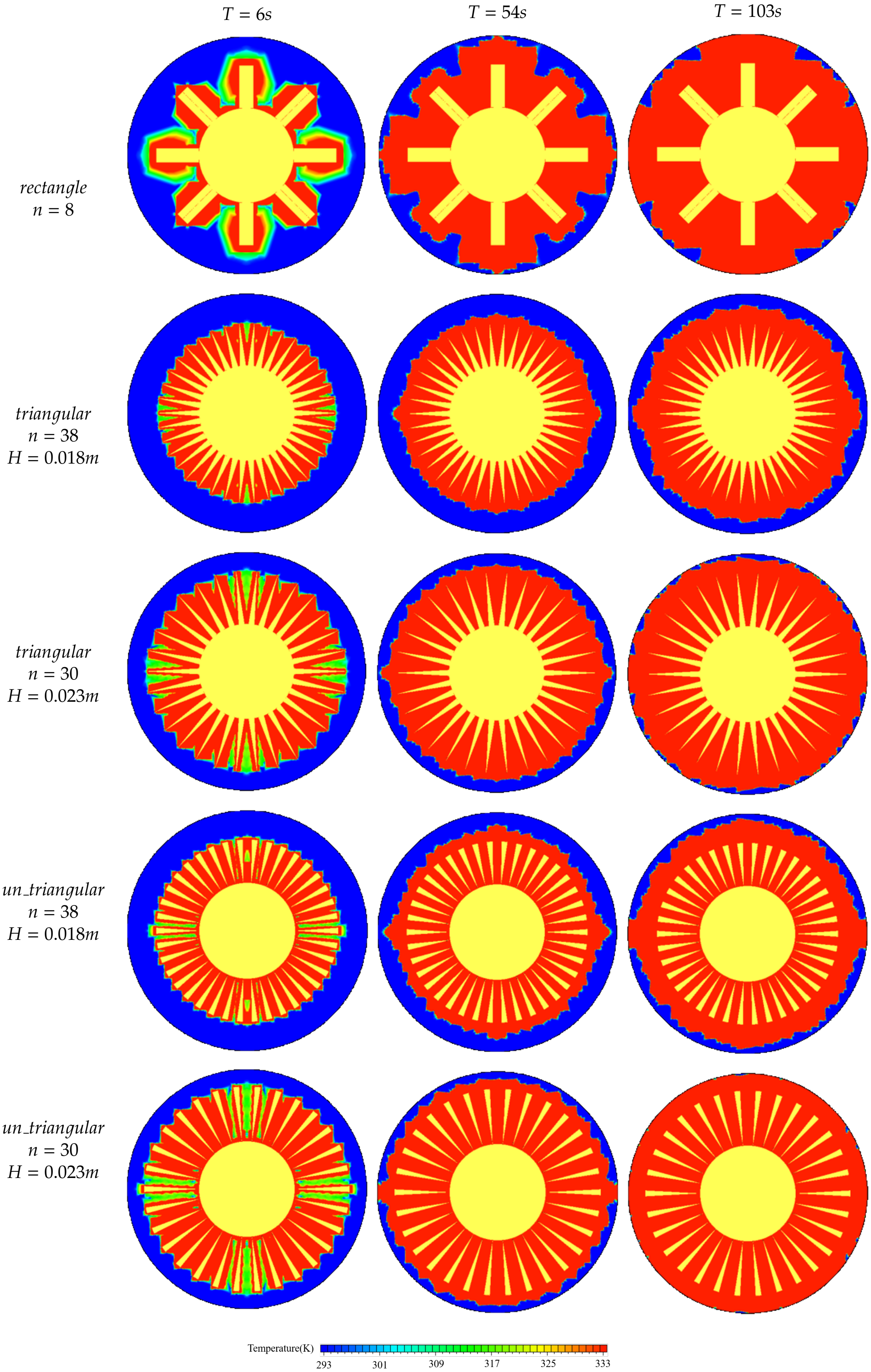

Figure 34: The temperature field under the condition of the same fin area(8*0.018*0.006)

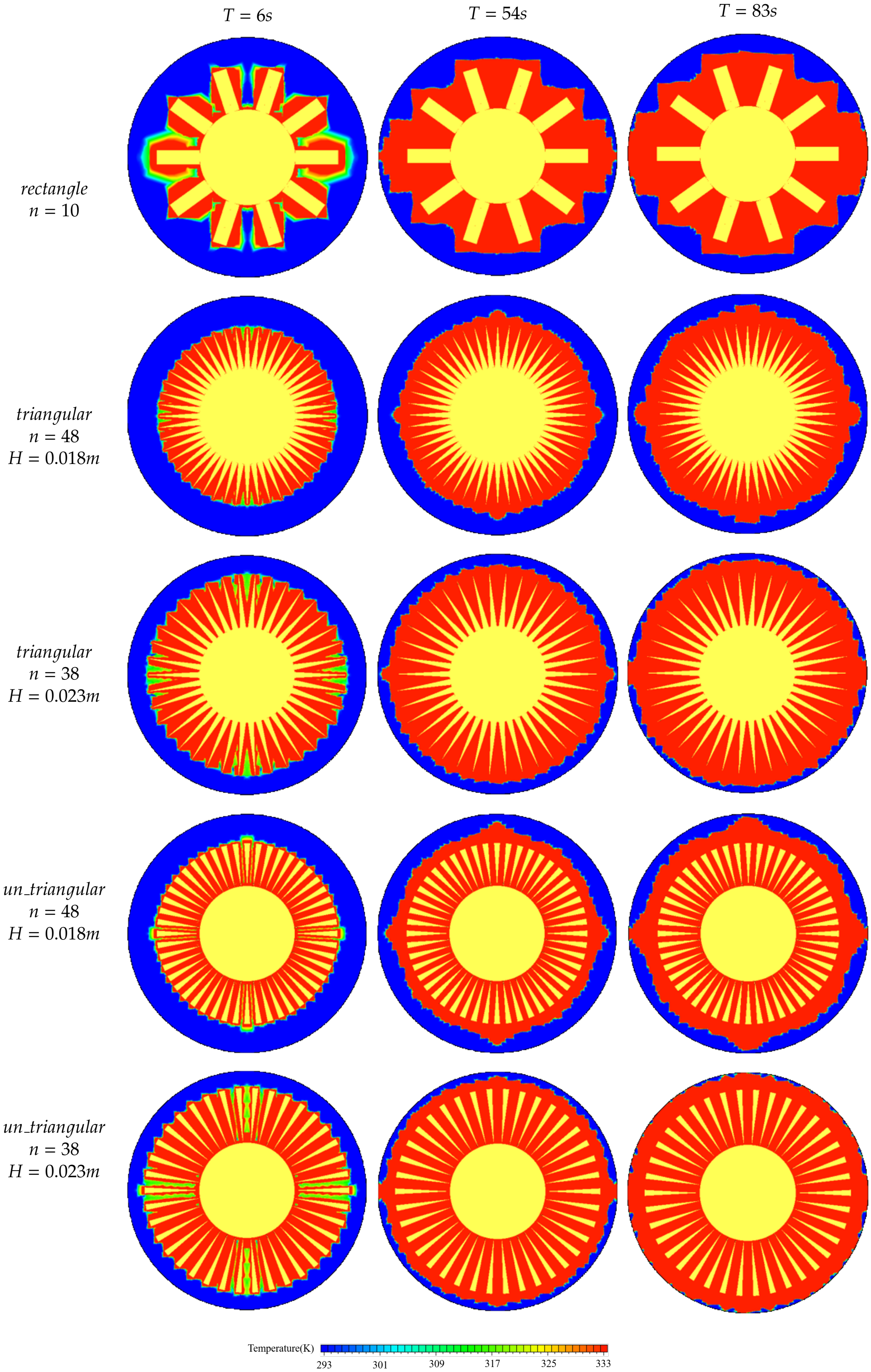

Figure 35: The temperature field under the condition of the same fin area(10*0.018*0.006)

5. Conclusion

This paper explores the heat transfer process of solid-state phase change materials through numerical investigations and proposes a comprehensive method for evaluating the performance of thermal storage systems with added fins. Specifically focusing on triangular fins, the impact of fin quantity, size, and arrangement on system performance was analyzed, leading to the following conclusions:

(1) This paper proposes a heat transfer model that employs a differential approach to analyze the cross-section of the overall phase change system and progressively analyze individual elements. In contrast to previous studies, this model eliminates the reliance on complex control equations and boundary conditions, avoiding the need for cumbersome solving processes. By utilizing the concept of dynamic programming, the heat transfer conditions from the previous time step are recursively calculated. Experimental results demonstrate that the proposed heat transfer model maintains stability during the heat transfer process under different time steps and grid sizes, with errors not exceeding 1%. Furthermore, compared to simulation results from other studies, the proposed heat transfer model exhibits minimal discrepancies, the average error is less than 2%.

(2) The number of fins has a significant impact on the thermal performance of phase change materials, particularly when triangular fins are added. In particular, when the number of fins is small, increasing the number of fins leads to a rapid decrease in the overall heat storage time. However, as the number of fins continues to increase, its influence on the overall heat storage time diminishes gradually. Therefore, it can be concluded that the impact of the number of fins on the overall heat storage time diminishes gradually as the number of fins increases.

(3) Under the condition that the number of triangular fins remains unchanged, changing the size of the triangular fins will affect the heat transfer performance. The experimental results show that increasing the height of the fin increases the heat transfer performance. By optimizing the fins confinement relationship, the fin area can be minimized while guaranteeing high heat transfer efficiency. In the optimal arrangement, when the height of the regular triangular fin is equal to the height of the rectangular fin, the evaluation value is 1.82, which is 3.8% higher than the optimal arrangement of rectangular fin.

(4) The layout of the inverted triangle fins is designed according to the analysis of the heat transfer distance field. In the case of the same fin size, the inverted triangle fin, which has a larger radiation range at the top, has a shorter heat transfer time. With the increase of fin height, the performance evaluation value of inverted triangle fin gradually becomes better than that of the positive triangle fin. The two types of triangular fins reached the optimal value of performance evaluation when the number of fins was 16, where the height of the positive triangular fin was $0.03m$ and the size of the inverted triangular fin was $0.029m$. It is worth noting that the best evaluation value of the inverted triangle fin is 17.3% higher than that of the positive triangle fin, indicating that the inverted triangle fin is a better choice in terms of high heat storage performance.

References

[1] Ammar M Abdulateef, Sohif Mat, Kamaruzzaman Sopian, Jasim Abdulateef and Ali A Gitan, Experimental and computational study of melting phase-change material in a triplex tube heat exchanger with longitudinal/triangular fins, *Solar Energy* **155** (2017), 142–153.

[2] Ci Ao, Suying Yan, Wenqi Hu, Long Zhao and Yuting Wu, Heat transfer analysis of a PCM in shell-and-tube thermal energy storage unit with different V-shaped fin structures, *Applied Thermal Engineering* **216** (2022), 119079.

[3] Ci Ao, Suying Yan, Xiaoyan Zhao, Na Zhang and Yuting Wu, Design optimization of a novel annular fin on a latent heat storage device for building heating, *Journal of Energy Storage* **64** (2023), 107124.

[4] A Valan Arasu and Arun S Mujumdar, Numerical study on melting of paraffin wax with Al2O3 in a square enclosure, *International Communications in Heat and Mass Transfer* **39** (2012), 8–16.

[5] Laura Colla, Laura Fedele, Simone Mancin, Ludovico Danza and Oronzio Manca, Nano-PCMs for enhanced energy storage and passive cooling applications, *Applied Thermal Engineering* **110** (2017), 584–589.

[6] Alicia Crespo, Camila Barreneche, Mercedes Ibarra and Werner Platzer, Latent thermal energy storage for solar process heat applications at medium-high temperatures–A review, *Solar Energy* **192** (2019), 3–34.

[7] Mohamed Amine Dekhil, Jules Voguelin Simo Tala, Odin Bulliard-Sauret and Daniel Bougeard, Numerical analysis of the performance enhancement of a latent heat storage shell and tube unit using finned tubes during melting and solidification, *Applied Thermal Engineering* **192** (2021), 116866.

[8] AA Ghoneim and SA Klein, The effect of phase-change material properties on the performance of solar air-based heating systems, *Solar Energy* **42** (1989), 441–447.

[9] Kh Hosseinzadeh, M Alizadeh and DD Ganji, Solidification process of hybrid nano-enhanced phase change material in a LHTESS with tree-like branching fin in the presence of thermal radiation, *Journal of Molecular Liquids* **275** (2019), 909–925.

[10] Xinyu Huang and Shouguang Yao, Solidification performance of new trapezoidal longitudinal fins in latent heat thermal energy storage, *Case Studies in Thermal Engineering* **26** (2021), 101110.

[11] Babak Kamkari and Dominic Groulx, Experimental investigation of melting behaviour of phase change material in finned rectangular enclosures under different inclination angles, *Experimental Thermal and Fluid Science* **97** (2018), 94–108.

[12] Ramin Karami and Babak Kamkari, Experimental investigation of the effect of perforated fins on thermal performance enhancement of vertical shell and tube latent heat energy storage systems, *Energy Conversion and Management* **210** (2020), 112679.

[13] JM Khodadadi and SF Hosseinizadeh, Nanoparticle-enhanced phase change materials (NEPCM) with great potential for improved thermal energy storage, *International communications in heat and mass transfer* **34** (2007), 534–543.

[14] Timothy J Kucharski, Nicola Ferralis, Alexie M Kolpak, Jennie O Zheng, Daniel G Nocera and Jeffrey C Grossman, Templated assembly of photoswitches significantly increases the energy-storage capacity of solar thermal fuels, *Nature chemistry* **6** (2014), 441–447.

[15] Yaxue Lin, Yuting Jia, Guruprasad Alva and Guiyin Fang, Review on thermal conductivity enhancement, thermal properties and applications of phase change materials in thermal energy storage, *Renewable and sustainable energy reviews* **82** (2018), 2730–2742.

[16] MD Muhammad, O Badr and H Yeung, Validation of a CFD melting and solidification model for phase change in vertical cylinders, *Numerical Heat Transfer, Part A: Applications* **68** (2015), 501–511.

[17] Seong Hyun Park, Yong Gap Park and Man Yeong Ha, A numerical study on the effect of the number and arrangement of tubes on the melting performance of phase change material in a multi-tube latent thermal energy storage system, *Journal of Energy Storage* **32** (2020), 101780.

[18] Alberto Pizzolato, Ashesh Sharma, Kurt Maute, Adriano Sciacovelli and Vittorio Verda, Design of effective fins for fast PCM melting and solidification in shell-and-tube latent heat thermal energy storage through topology optimization, *Applied Energy* **208** (2017), 210–227.

[19] Yinghong Qin, Numerical modeling of energy storage unit during freezing of paraffin utilizing Al2O3 nanoparticles and Y-shape fin, *Journal of Energy Storage* **44** (2021), 103452.

[20] Fan Ren, Jun Du, Yufei Cai, Jing Guo, Yong Liu, Dongxing Zhang and Menghan Li, Study on thermal performance of a new optimized snowflake longitudinal fin in vertical latent heat storage, *Journal of Energy Storage* **50** (2022), 104165.

[21] A Rozenfeld, Y Kozak, T Rozenfeld and G Ziskind, Experimental demonstration, modeling and analysis of a novel latent-heat thermal energy storage unit with a helical fin, *International Journal of Heat and Mass Transfer* **110** (2017), 692–709.

[22] Yongliang Shen, Abdur Rehman Mazhar, Pengwei Zhang and Shuli Liu, Investigation of the volume impact on cascaded latent heat storage system by coupling genetic algorithm and CFD simulation, *Journal of Energy Storage* **48** (2022), 104065.

[23] Yongliang Shen, Abdur Rehman Mazhar, Pengwei Zhang and Shuli Liu, Structure optimization of tree-shaped fins for improving the thermodynamic performance in latent heat storage, *International Journal of Thermal Sciences* **184** (2023), 108003.

[24] Zichen Wang, Zhuqian Zhang, Li Jia and Lixin Yang, Paraffin and paraffin/aluminum foam composite phase change material heat storage experimental study based on thermal management of Li-ion battery, *Applied Thermal Engineering* **78** (2015), 428–436.

[25] Shuying Wu, Hua Wang, Song Xiao and Dongsheng Zhu, Numerical simulation on thermal energy storage behavior of Cu/paraffin nanofluids PCMs, *Procedia Engineering* **31** (2012), 240–244.

[26] Wei-Biao Ye, Hong-Ju Guo, Si-Min Huang and Yu-Xiang Hong, Research on melting and solidification processes for enhanced double tubes with constant wall temperature/wall heat flux, *Heat Transfer—Asian Research* **47** (2018), 583–599.

[27] Xialan Zhang, Qilang Lin, Huijun Luo and Shiyuan Luo, Three-dimensional graphitic hierarchical porous carbon/stearic acid composite as shape-stabilized phase change material for thermal energy storage, *Applied Energy* **260** (2020), 114278.

[28] Kerun Liu, Yitian Zhang and Chaoran Guo, Structural Optimization of Heat Transfer Fins in the Energy Storage System, *Highlights in Science*, *Engineering and Technology* 71 (2023), 345–356.